Covalently Mercurated 6-Phenylcarbazole Residues Promote Hybridization of Triplex-Forming Oligonucleotides

Dattatraya Uttam Ukale[a] and Tuomas Lönnberg*[a]

[a] Dr. D. U. Ukale, Prof. T. Lönnberg
Department of Chemistry
University of Turku
Henrikinkatu 2, 20500 Turku, Finland
E-mail: tuanlo@utu.fi

Supporting information for this article is given via a link at the end of the document.

Abstract: Homothymidine DNA oligonucleotides bearing a 3´-terminal 6-phenyl-9*H*-carbazole C-nucleoside, mercurated at position 1, 8 or both, were synthesized and tested for their potential to form triple helices with homoadenine•homothymine duplexes. The monomercurated triplex-forming oligonucleotides favored hybridization with fully matched double helices and in some cases considerable increase of the melting temperature could be attributed to Hoogsteen-type Hg(II)-mediated interaction with the homoadenine strand. The dimercurated one, on the other hand, favored hybridization with double helices placing a homo mispair opposite to the carbazole residue, suggesting that simultaneous coordination of each of the two Hg(II) ions to a different strand is only possible in the absence of competition from Watson—Crick base pairing.

Introduction

Triplex-forming oligonucleotides (TFOs) offer an elegant approach for targeting genomic DNA[1–6] but suffer from a relatively low hybridization affinity.[7–10] This problem has been tackled by introduction of positive charges,[11,12] removal of negative charges,[13] rigidification[14–19] and conjugation with various triplex-stabilizing groups[20–25]. Metal-mediated base pairing, studied extensively in a double-helical context[26–32], also appears feasible but so far only a handful of cases have been reported[33–44].

We have shown that a dinuclear Hg(II)-mediated base triple between one modified and two canonical nucleobases can greatly increase both Hoogsteen and Watson—Crick melting temperatures of a triple-helical oligonucleotide.[45] As the modified nucleobase was incorporated in the middle (Watson) strand of the triple helix, the mode presented is not directly applicable to targeting genomic DNA. One could, however, envision an extended metallated nucleobase surrogate, the metal centers of which could simultaneously bind with both partners of a Watson—Crick base pair. Modified nucleobases capable of forming analogous hydrogen-bonded base triples have been described in the literature (Figure 1).[46–51] We realized that 1,8-dimercury-6-phenyl-9*H*-carbazole, a dinuclear organomercury nucleobase recently studied by us within double-helical oligonucleotides[52,53], might be able to form dinuclear Hg(II)-mediated base triples with canonical Watson—Crick base pairs. Specifically, the distance between the two Hg(II) ions appears suitable for simultaneous coordination to an adenine- or guanine-N7 within the homopurine strand and a thymine-O4 or cytosine-N4 within the homopyrimidine strand. We present herein a thorough study on the triplex-forming preferences of a homothymine oligonucleotide incorporating a 5′-terminal 1,8-dimercury-6-phenyl-9*H*-carbazole residue, as well as its 1- or 8-monomercurated counterparts.

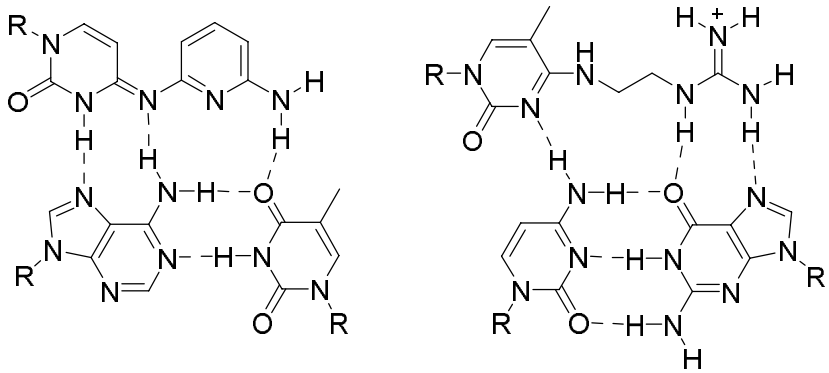

Figure 1. Examples of hydrogen-bonded base triples with potential to stabilize triple helices.

Results and Discussion

Oligonucleotide synthesis

The sequences of the oligonucleotides used in the present study are summarized in Table 1. Constituent strands of the target duplexes (ON1 and ON2) were commercial products apart from the 7-deazaadenine- and 7-deazaguanine-modified ON2da and ON2dg, which were synthesized by an automated DNA/RNA synthesizer from commercially available building blocks following standard protocols. The triplex-forming 15-mer homothymine oligonucleotide ON3z incorporating a 3´-terminal 6-phenyl-9*H*-carbazole residue, in turn, was assembled on a CPG-supported universal linker employing an extended (300 s) coupling time for the modified phosphoramidite building block[52]. Mercuration of ON3z was carried out by incubation in an aqueous solution of mercuric acetate and sodium acetate and the products were isolated by RP-HPLC using an ethanethiol-containing eluent to suppress non-specific coordination of Hg(II). The chromatogram of the crude product mixture revealed formation of three distinct products with longer retention times than the starting material. Mass spectrometric analysis identified the slowest-eluting product as the dimercurated oligonucleotide ON3z-Hg2, while both of the faster eluting products turned out to be monomercurated. With related oligonucleotides[52], the 6-phenyl-9*H*-carbazole residue has previously been established as the site of mercuration by a P1 nuclease digestion assay. The two monomercurated products (ON3z-Hg1a and ON3z-Hg1b for the faster- and slower-eluting isomers) in all likelihood contained either a 1-mercury-6-phenyl-9*H*-carbazole or an 8-mercury-6-phenyl-9*H*-carbazole residue at their 3´-termini but attempts to characterize the structures of these oligonucleotides in more detail were unsuccessful. Finally, all synthesized oligonucleotides were quantified UV spectrophotometrically.

Table 1. Oligonucleotides used in the present study.

Oligonucleotide	Sequence[a]
ON1a	5′-d(GAT TTT TTT TTT TTT TTG C)-3′
ON1c	5′-d(GCT TTT TTT TTT TTT TTG C)-3′
ON1g	5′-d(GGT TTT TTT TTT TTT TTG C)-3′
ON1t	5′-d(GTT TTT TTT TTT TTT TTG C)-3′
ON2a	5′-d(GCA AAA AAA AAA AAA AAA C)-3′
ON2c	5′-d(GCA AAA AAA AAA AAA AAC C)-3′
ON2g	5′-d(GCA AAA AAA AAA AAA AAG C)-3′
ON2t	5′-d(GCA AAA AAA AAA AAA AAT C)-3′
ON2da	5′-d(GCA AAA AAA AAA AAA AAA* C)-3′
ON2dg	5′-d(GCA AAA AAA AAA AAA AAG* C)-3′
ON3z	5′-d(TTT TTT TTT TTT TTT Z)-3′
ON3z-Hg1a	5′-d(TTT TTT TTT TTT TTT Z^{Hg1a})-3′
ON3z-Hg1b	5′-d(TTT TTT TTT TTT TTT Z^{Hg1b})-3′
ON3z-Hg2	5′-d(TTT TTT TTT TTT TTT Z^{Hg2})-3′

[a] A* refers to 7-deazaadenine, G* to 7-deazaguanine, Z to 6-phenyl-9*H*-carbazole, Z^{Hg1a} and Z^{Hg1b} to the monomercurated 6-phenyl-9*H*-carbazole in the faster and more slowly eluting monomercurated oligonucleotides ON3z-Hg1a and ON3z-Hg1b and Z^{Hg2} to 1,8-dimercuri-6-phenyl-9*H*-carbazole. In each sequence, the residue varied in the hybridization experiments has been underlined.

Hybridization studies

Hybridization affinity of the TFOs for various double helices was quantified by an assay used previously for similar studies on TFOs bearing a 3′-terminal 5-mercuricytosine or -uracil (Figure 2).[39] The study was limited to homoadenine•homothymine target duplexes to allow triplex formation at physiological pH but CG base pairs were included at both ends of the duplexes to ensure sufficient thermal stability and antiparallel secondary structure. The variable target base pair was located immediately upstream of the homothymine sequence. In addition to all four canonical Watson-Crick base pairs, homo base pairs of canonical nucleobases were also tested, as well as 7-deazaadenine•thymine and 7-deazaguanine•cytosine base pairs (with the 7-deazapurine residue in the homopurine strand). UV melting profiles of the various triplexes were acquired at pH 7.4 (20 mM cacodylate buffer), a 10 mM concentration of Mg(II) and an ionic strength of 0.10 M (adjusted

with sodium perchlorate). In each sample, all of the three oligonucleotides were present at a 1.0 μM concentration.

5´-d(G<u>X</u> TTT TTT TTT TTT TTT GC)-3´
3´-d(C<u>Y</u> AAA AAA AAA AAA AAA CG)-5´
3´-d(<u>Z</u> TTT TTT TTT TTT TTT)-5´

Figure 2. Outline of the hybridization assay used. Base X is any canonical nucleobase, Y is any canonical nucleobase, 7-deaazaadenine or 7-deazaguanine and Z is 6-phenyl-9*H*-carbazole, 1-mercuri-6-phenyl-9*H*-carbazole, 8-mercuri-6-phenyl-9*H*-carbazole or 1,8-dimercuri-6-phenyl-9*H*-carbazole.

Figure 3 shows UV melting profiles of triplexes ON1t•ON2a*ON3z, ON1t•ON2da*ON3z, ON1t•ON2a*ON3z-Hg1b and ON1t•ON2da*ON3z-Hg1b as representative examples (all melting profiles are provided as Figures S6—S49 in the Supporting Information). All of the triplexes studied exhibited biphasic or triphasic sigmoidal melting profiles. In most cases, the denaturation and renaturation curves overlapped nearly perfectly but with ON1t•ON2a*ON3z-Hg2, ON1t•ON2da*ON3z-Hg2, ON1c•ON2dg*ON3z-Hg2 and ON1a•ON2t*ON3z-Hg1b considerable hysteresis was observed. Melting temperatures were obtained by fitting the melting curves to a biphasic model (Equation 1), ignoring the event associated with the smallest hyperchromicity.

$$A/A_{90} = a_{low} + b_{low}T + \left[\left(a_{high} + b_{high}T\right) - \left(a_{low} + b_{low}T\right)\right]\left[\frac{p}{1+10^{(T_{m,HG}-T)h_{HG}}} + \frac{1-p}{1+10^{(T_{m,WC}-T)h_{WC}}}\right] \quad (1)$$

A and A_{90} are measured absorbances at a given temperature and at 90 °C. a_{low} and b_{low} are the offset and slope of the "low-temperature" baseline and a_{high} and b_{high} the corresponding values for the "high-temperature" baseline. These terms were needed to account for the fact that neither of the baselines are necessarily horizontal. p is the fraction of hyperchromicity associated with the Hoogsteen melting (relative to overall hyperchromicity). $T_{m,HG}$ and $T_{m,WC}$ are the Hoogsteen and Watson—Crick melting temperatures and h_{HG} and h_{WC} the slopes of the melting curves at these temperatures. Hoogsteen and Watson—Crick melting temperatures of all triplexes are summarized in Table S1 in the Supporting information.

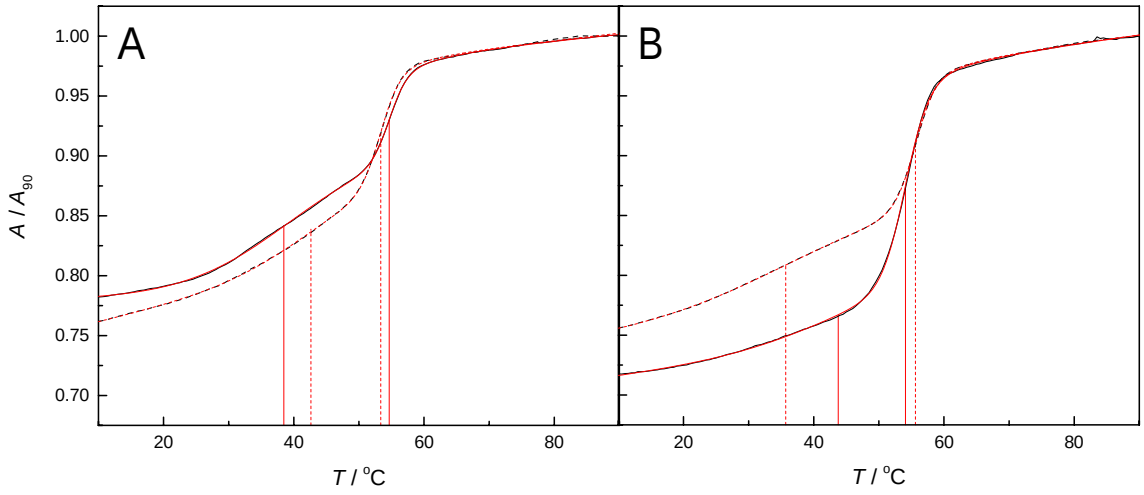

Figure 3. A) UV melting profiles (black line) and their fitting to Equation 1 (red line) of ON1t•ON2a*ON3z (solid line) and ON1t•ON2da*ON3z (dashed line); B) UV melting profiles (black line) and their fitting to Equation 1 (red line) of ON1t•ON2a*ON3z-Hg1b (solid line) and ON1t•ON2da*ON3z-Hg1b (dashed line); pH = 7.4 (20 mM cacodylate buffer); [oligonucleotides] =1.0 μM; [Mg(II)] = 10 mM; $I(NaClO_4)$ = 0.10 M. The vertical lines indicate the melting temperatures obtained by fitting to Equation 1.

Watson—Crick melting temperatures of the triplexes studied ranged from 55 to 58 °C with the matched target duplexes and from 50 to 53 °C with the mismatched target duplexes, being largely insensitive to the identity of the TFO (data not shown). The Hoogsteen melting temperatures, in turn, were highly dependent on both the target duplex and the TFO, especially with the mercurated TFOs (Figure 4). Determination of the Hoogsteen melting temperatures was complicated not only by overlapping with Watson—Crick melting temperatures in some cases but also by the more gradual transition. Accordingly, some values could not be obtained reliably.

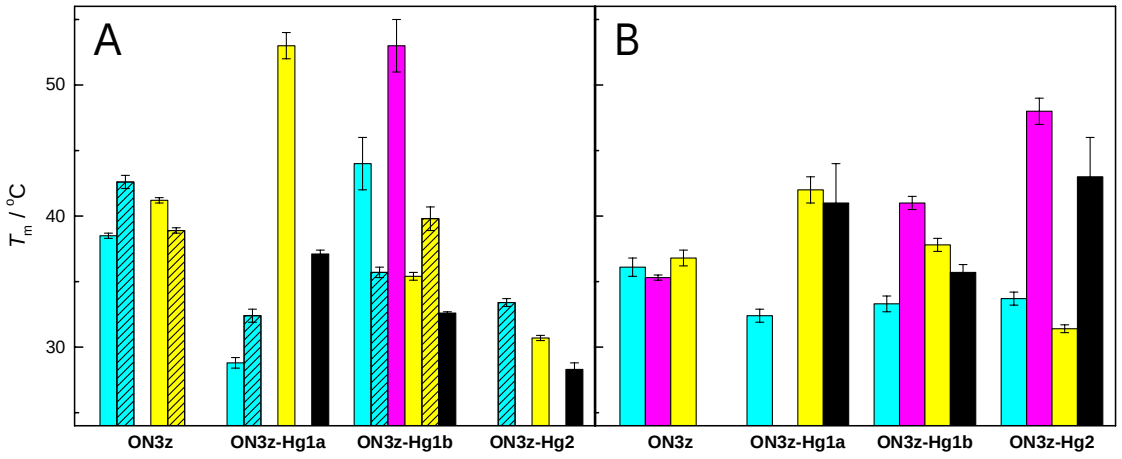

Figure 4. Hoogsteen melting temperatures of triplexes formed by the modified TFOs with target duplexes A) ON1t•ON2a (cyan), ON1t•ON2da (hashed cyan), ON1g•ON2c (magenta), ON1c•ON2g (yellow), ON1c•ON2dg (hashed yellow) and ON1a•ON2t (black) and B) ON1a•ON2a (cyan), ON1c•ON2c (magenta), ON1g•ON2g (yellow) and ON1t•ON2t (black); pH = 7.4 (20 mM cacodylate buffer); [oligonucleotides] =1.0 μM; [Mg(II)] = 10 mM; $I(NaClO_4)$ = 0.10 M.

Hoogsteen melting temperatures of the triplexes formed by the unmercurated TFO ON3z fell into two distinct categories: approximately 38—43 °C with fully matched target duplexes and approximately 35—37 °C with duplexes featuring a mispair at the target site. In other words, the hybridization affinity of ON3z depended more on intact base stacking of the target duplex than on the identity of the target nucleobase within the homopurine strand. Comparison of triplexes ON1t•ON2a*ON3z and ON1c•ON2g*ON3z with ON1t•ON2da*ON3z and ON1c•ON2dg*ON3z, replacing the purine base at the target site with its 7-deaza analog, makes this point particularly evident. Removal of the purine N7 would be expected to considerably destabilize the triplex if the modified 6-phenyl-9*H*-carbazole base was involved in Hoogsteen-type hydrogen bonding. This was, however, not the case and between ON1t•ON2a*ON3z and ON1t•ON2da*ON3z a 4 °C increase in the Hoogsteen melting temperature was actually observed. The sensitivity to intact base stacking and the insensitivity to the hydrogen bonding pattern at the target site both suggest that the 6-phenyl-9*H*-carbazole base exerts its triplex-stabilizing effect mainly through intercalation.

The faster-eluting monomercurated TFO ON3z-Hg1a favored guanine and, in the case mismatched target duplexes, thymine, as the target nucleobase within the homopurine strand. With ON1c•ON2g*ON3z-Hg1a, the Hoogsteen melting temperature was 53.0 °C, more than 10 °C higher than with its unmercurated counterpart ON1c•ON2g*ON3z. Unfortunately, the impact of replacing the guanine in the homopurine

strand with 7-deazaguanine remained obscure as the Hoogsteen melting temperature of triplex ON1c•ON2dg*ON3z-Hg1a could not be determined reliably. Therefore, we cannot firmly establish the site of mercuration of the carbazole as either C1 or C8, although the very low Hoogsteen melting temperature of triplex ON1t•ON2a*ON3z-Hg1a would be more consistent with the latter. In contrast to ON3z, integrity of the base stack at the target site was not absolutely critical to triplex formation, as evidenced by the relatively high Hoogsteen melting temperatures of ON1g•ON2g*ON3z-Hg1a and ON1t•ON2t*ON3z-Hg1a (42 and 41 °C, respectively). Between target duplexes featuring thymine in the homopurine strand, the mismatched ON1t•ON2t was actually somewhat favored over the matched ON1a•ON2t. This observation could be explained by interaction of the monomercurated base with the Watson—Crick face of the thymine. In the case of the TT mispair, the Watson—Crick face of thymine would be more readily available for Hg(II)-mediated base pairing as no disruption of a canonical base pair would be involved.

The more slowly eluting monomercurated TFO ON3z-Hg1b formed the most stable triplexes with fully matched target duplexes incorporating adenine or, especially, cytosine at the target site of the homopurine strand (44 and 53 °C, respectively). With mismatched target duplexes, no clear preference for any particular nucleobase was observed, the Hoogsteen melting temperatures ranging from 33 to 41 °C. Replacing the target site adenine in the homopurine strand with 7-deazaadenine resulted in an 8 °C destabilization, consistent with Hg(II) coordination to adenine N7 as the reason behind the high stability of the ON1t•ON2a*ON3z-Hg1b triplex. In contrast, the Hoogsteen melting temperature of ON1c•ON2g*ON3z-Hg1b was more than 8 °C lower than that of ON1t•ON2a*ON3z-Hg1b and actually more than 4 °C lower than that of its 7-deazaguanine counterpart ON1c•ON2dg*ON3z-Hg1b. These results could be explained tentatively by the carbazole moiety of ON3z-Hg1b being mercurated at C1 and (deprotonated) cytosine-N4 being preferred over purine-N7 as the Hg(II) coordination site. Besides cytosine[54], this type of coordination has been reported with adenine[55]. Accordingly, the most stable triplex is ON1g•ON2c*ON3z-Hg1b, with cytosine in the homopurine strand (Figure 5A). In ON1c•ON2g*ON3z-Hg1b and ON1c•ON2dg*ON3z-Hg1b, Hg(II) would also be coordinated to cytosine but such coordination would be less conducive to triplex formation as the cytosine is placed in the homopyrimidine strand. Conflicts between stability of a metal-mediated base pair at monomer level and melting temperature of the corresponding duplex have been reported previously[56–58] and usually attributed to geometric incompatibility. Finally, triplex ON1t•ON2a*ON3z-Hg1b, lacking a cytosine, would instead involve the expected coordination to adenine-N7 within the homopurine strand (Figure 5B).

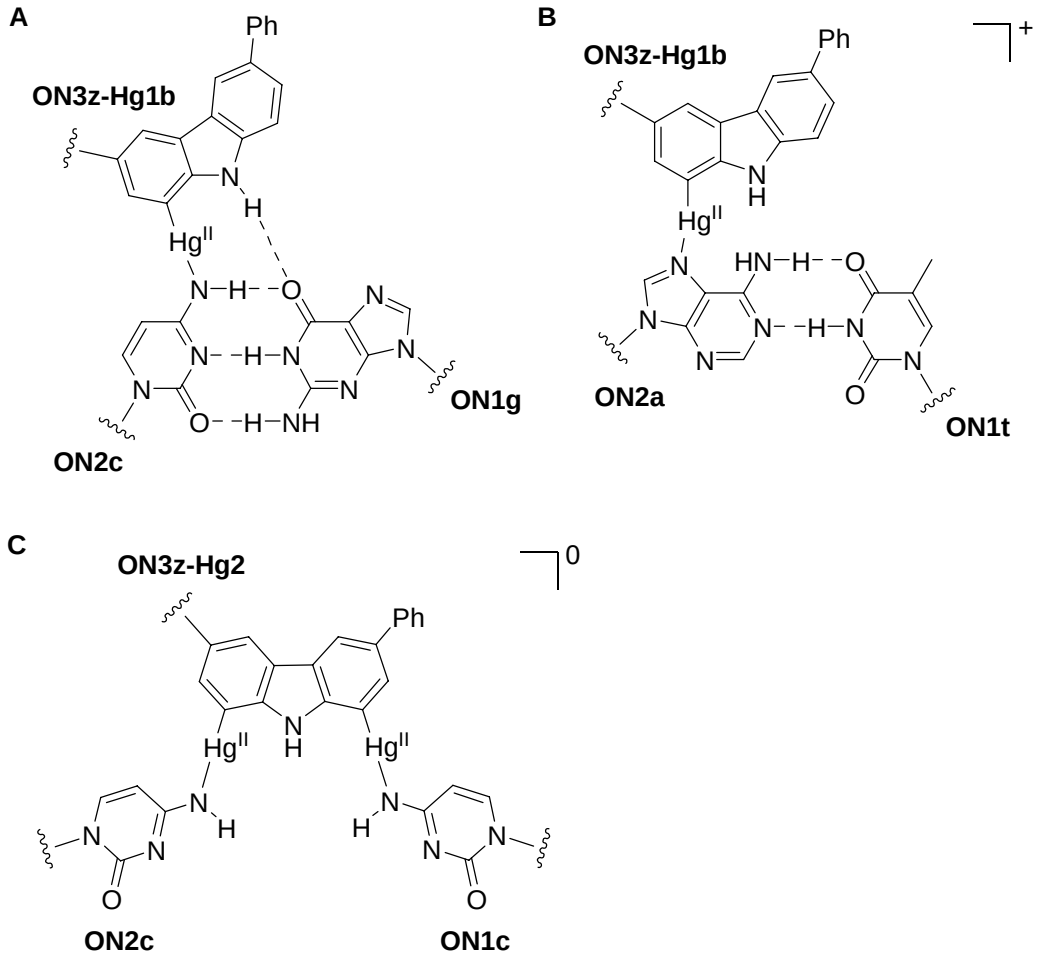

Figure 5. Tentative structures of Hg(II)-mediated base triples within the oligonucleotide triplexes A) ON1g•ON2c*ON3z-Hg1b, B) ON1t•ON2a*ON3z-Hg1b and C) ON1c•ON2c*ON3z-Hg2.

In contrast to all of the other TFOs studied, the dimercurated TFO ON3z-Hg2 actually favored hybridization with mismatched rather than matched duplexes, especially those with a CC or TT mispair at the target site. Hoogsteen melting temperatures of the triplexes formed by ON3z-Hg2 with the matched target duplexes were among the lowest observed (less than 34 °C) or could not be determined at all. ON1c•ON2c*ON3z-Hg2, on the other hand, was the most stable of all the mismatched triplexes studied (T_m = 48 °C). The unexpected preference of ON3z-Hg2 for the mismatched target duplexes could be understood if the two Hg(II) ions of 1,8-dimercuri-6-phenyl-9*H*-carbazole coordinate to two separate nucleobases in a way that prevents them from forming a base pair with each other. In such a case, formation of a Hg(II)-mediated base triple with a Watson—Crick or even a stable wobble base pair would come at the cost of losing most or all of the original hydrogen bonds. According to this reasoning, the highest Hoogsteen melting temperatures would be observed with triplexes placing the 1,8-dimercuri-6-phenyl-9*H*-carbazole against the weakest mispairs. Of the homo base pairs tested, CC is the weakest one[59] and, indeed, the corresponding triplex

ON1c•ON2c*ON3z-Hg2 exhibited the highest Hoogsteen melting temperature. Hg(II) coordination could take place at either N3 or N4 and the data at hand does not allow distinction between these two binding modes. Indeed, N4 vs. N3 dichotomy of C—Hg(II)—T base pairs within double-helical oligonucleotides has been reported and found to be sensitive to subtle differences in the duplex geometry.[54,60,61] In the present case, neither binding mode seems possible without considerable opening of the CC mispair. We have chosen to present the charge-neutral triple with N4 coordination to both cytosines (Figure 5C) as the angle between the N-glycosidic bonds is somewhat smaller in this structure than the one involving N3 coordination.

Folding of the oligonucleotide triplexes into the expected secondary structures was verified by circular dichroism (CD) spectropolarimetry. Sample preparation was identical to the UV melting experiments and the spectra were acquired at 10 °C intervals over a range of 10—90 °C. The spectra for triplex ON1t•ON2a*ON3z-Hg1b are presented in Figure 6 as an illustrative example and all other spectra in the Supporting Information. At the low end of the temperature range, all spectra showed negative Cotton effects at λ = 248 nm and positive ones at λ = 260 and λ = 284 nm, characteristic of homopyrimidine•homopurine*homopyrimidine triple helices. The first two Cotton effects diminished with increasing temperature, while the third one shifted towards shorter wavelengths, consistent with dissociation of the TFO, followed by unwinding of the remaining Watson—Crick double helix.

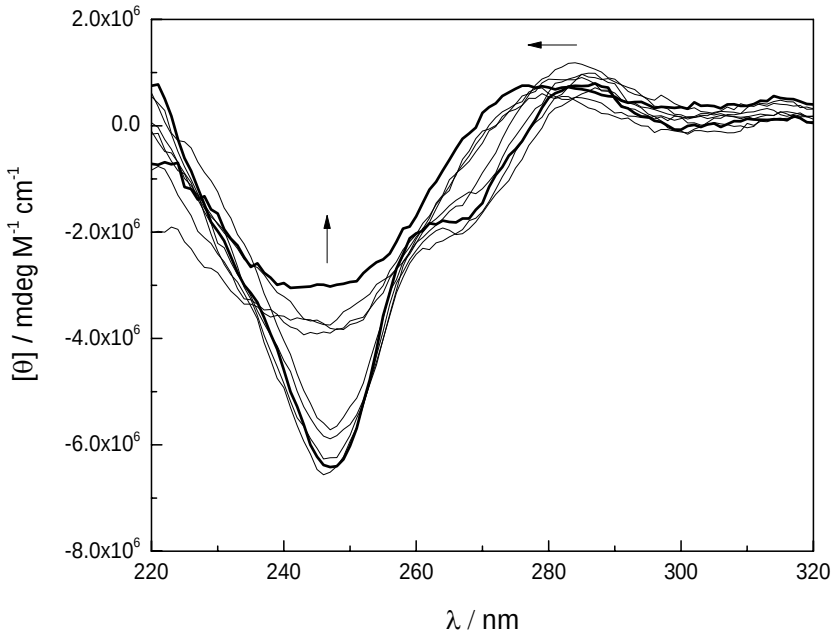

Figure 6. CD spectra of triplex ON1t•ON2a*ON3z-Hg1b, recorded at 10 °C intervals over a range of 10—90 °C; pH = 7.4 (20 mM cacodylate buffer); [oligonucleotides] =1.0 μM; [Mg(II)] = 10 mM; *I*($NaClO_4$) = 0.10 M. Spectra acquired at 10 and 90 °C are indicated by thicker lines and thermal shifts of the minima and maxima by arrows.

Plotting of the most intensive Cotton effect (the one at λ = 248 nm) as a function of temperature gave biphasic sigmoidal CD melting profiles. Fitting of these profiles to a biphasic model (essentially Equation 1 but with horizontal baselines, Figures S50—S129 in the Supporting Information) allowed estimation of two melting temperatures. However, the limited number of data points made this estimation rather rough and in many cases the Hoogsteen melting temperature could not be obtained at all. The higher melting temperature, assigned as the Watson—Crick one, agreed in most cases reasonably well with the one obtained from the UV melting profiles (Table S1 in the Supporting Information). The lower CD melting temperature showed much greater variation but in most cases was nevertheless within error limits from its UV counterpart.

Conclusion

3′-Terminal mercurated 6-phenyl-9*H*-carbazole C-nucleoside residues were found to promote hybridization of homothymidine TFOs with double-helical targets. The greatest stabilization could be assigned to

coordination of Hg(II) to cytosine, tentatively the exocyclic N4. In contrast to its 1- or 8-monomercurated counterparts, 1,8-dimercuri-6-phenyl-9*H*-carbazole did not promote hybridization with fully matched double helices but instead preferred targets featuring a homo mispair opposite to this modified residue. Evidently, the carbazole scaffold is not sufficiently long to allow simultaneous coordination of the two Hg(II) ions to both partners of a Watson—Crick base pair, at least within a homopyrimidine•homopurine*homopyrimidine triple-helical environment.

Acknowledgements

We thank Dr. Petri Tähtinen and Dr. Petteri Vainikka for fruitful discussions. Dr. Dattatraya Ukale gratefully recognizes financial support from Finnish Cultural Foundation.

Experimental

General methods

All reagents, as well as the unmodified oligonucleotides, were commercial products that were used as received. Freshly distilled triethylamine was for used for preparation of the HPLC elution buffers. Mass spectra were recorded on a Bruker microTOF-Q mass spectrometer.

Oligonucleotide synthesis

The triplex-forming DNA oligonucleotide ON3z, containing the modified 6-phenyl-9*H*-carbazole residue at its 3´-terminus, as well as the 7-deaza-modified target strands ON2da and ON2dg were synthesized by an Applied Biosystems 3400 automated DNA/RNA synthesizer on a CPG-supported universal linker. Standard phosphoramidite chemistry with 5-(benzylthio)-9*H*-tetrazole as the activator was employed, with coupling time of the 6-phenyl-9*H*-carbazole C-nucleoside building block[52] extended to 300 s. Based on trityl response, all couplings proceeded with normal efficiency. Cleavage from the solid support and deprotection of the phosphate and, in the case of ON2da and ON2dg, base moieties was achieved by incubation in 33 % aqueous ammonia at 55 °C overnight. Afterwards the supernatant was recovered, the remaining solid supports were washed with water and the combined solutions lyophilized. The crude products were purified by RP-HPLC on a Hypersil ODS C18 column (250 × 4.6 mm, 5 µm) eluting with a linear gradient (10—40 % over 20 min, flow rate = 1.0 mL min^{-1}) of MeCN in a 50 mM triethylammonium acetate buffer (pH = 7.0).

Synthesis of the mercurated TFOs ON3z-Hg1a, ON3z-Hg1b and ON3z-Hg2 was carried out by incubating ON3z (188 µM), $Hg(OAc)_2$ (4700 µM) and NaOAc (0.10 M) in 100 µL of water at 55 °C overnight. The progress of reaction was monitored by RP-HPLC on a Hypersil ODS C18 column (250 × 4.6 mm, 5 µm) eluting with a linear gradient (15—45 % over 30 min, flow rate = 1.0 mL min^{-1}) of MeCN in a 50 mM triethylammonium acetate buffer (pH = 7.0) containing ethanethiol (1 mM). When a satisfactory product distribution had been achieved, the reaction mixture was fractioned by RP-HPLC under the same conditions. Fractions containing the desired mercurated TFOs underwent a second round of purification by RP-HPLC on a Hypersil ODS C18 column (250 × 4.6 mm, 5 µm) eluting with a linear gradient of MeCN (10—40 % over 20 min, flow rate = 1.0 mL min^{-1}) in a 50 mM triethylammonium acetate buffer (pH = 7.0). Finally, all purified oligonucleotides were characterized by ESI-TOF mass spectrometry and quantified by UV spectrophotometry using molar absorptivities calculated by an implementation of the nearest-neighbors method. The previously determined[52] value of 124 000 L mol^{-1} cm^{-1} was used for the 6-phenyl-9*H*-carbazole residue and its mercurated derivatives.

UV melting experiments

UV melting profiles were recorded on a Perkin Elmer Lambda 35 UV spectrometer equipped with Peltier temperature control unit, using quartz cuvettes with 10 mm optical path length. The samples contained a 1 µM concentration of the appropriate oligonucleotides in 400 µL of 20 mM cacodylate buffer (pH 7.4). The Mg(II) concentration of the samples was adjusted to 10 mM with $Mg(ClO_4)_2$ and the ionic strength to 100 mM with $NaClO_4$. Before each experiment, the samples were annealed by heating up to 90 °C and allowing to slowly cool down to room temperature. All measurement were carried out between 10 and 90 °C with three 0.5 °C min^{-1} heating and cooling ramps, recording absorbance at 260 nm at 0.5 °C intervals. Melting temperatures were obtained by fitting the experimental data to Equation 1.

CD experiments

CD spectra were recorded on an Applied Photophysics Chirascan spctropolarimeter equipped with Peltier temperature control unit. The sample preparation and the cuvettes were identical to the those of the UV melting experiments. Spectra were acquired between 200 and 400 nm and 10 and 90 °C at 10 °C intervals. At each temperature, the samples were allowed to equilibrate for 120 s before recording the spectra.

Keywords: triple helix • oligonucleotides • mercury • organometallic compounds • coordination

References

[1] C. Helene, *Anticancer Drug Des.* 1991, *6*, 569–584.

[2] L. J. Maher, *Bioessays* 1992, *14*, 807–815.

[3] L. J. Maher, *Cancer Invest.* 1996, *14*, 66–82.

[4] M. M. Seidman, P. M. Glazer, *J. Clin. Invest.* 2003, *112*, 487–494.

[5] T. Ros, G. Spalluto, M. Prato, T. Saison-Behmoaras, A. Boutorine, B. Cacciari, *Curr. Med. Chem.* 2005, *12*, 71–88.

[6] A. Jain, G. Wang, K. M. Vasquez, *Biochimie* 2008, *90*, 1117–1130.

[7] N. T. Thuong, C. Hélène, *Angew. Chem. Int. Ed.* 1993, *32*, 666–690.

[8] S. Buchini, C. J. Leumann, *Curr. Opin. Chem. Biol.* 2003, *7*, 717–726.

[9] J. Robles, A. Grandas, E. Pedroso, F. J. Luque, R. Eritja, M. Orozco, *Curr. Org. Chem.* 2002, *6*, 1333–1368.

[10] K. R. Fox, *Curr. Med. Chem.* 2000, *7*, 17–37.

[11] M. L. Jain, P. Y. Bruice, I. E. Szabó, T. C. Bruice, *Chem. Rev.* 2012, *112*, 1284–1309.

[12] V. Tähtinen, A. Verhassel, J. Tuomela, P. Virta, *ChemBioChem* 2019, *20*, 3041–3051.

[13] V. V Demidov, M. D. Frank-Kamenetskii, *Methods* 2001, *23*, 108–122.

[14] E. Bernal-Méndez, C. J. Leumann, *J. Biol. Chem.* 2001, *276*, 35320–35327.

[15] Y. V Pabon-Martinez, Y. Xu, A. Villa, K. E. Lundin, S. Geny, C. H. Nguyen, E. B. Pedersen, P. T. Jorgensen, J. Wengel, L. Nilsson, C. I. E. Smith, R. Zain, *Sci. Rep.* 2017, *7*, 11043.

[16] S. Obika, T. Uneda, T. Sugimoto, D. Nanbu, T. Minami, T. Doi, T. Imanishi, *Bioorg. Med. Chem.* 2001, *9*, 1001–1011.

[17] H. Torigoe, Y. Hari, M. Sekiguchi, S. Obika, T. Imanishi, *J. Biol. Chem.* 2001, *276*, 2354–2360.

[18] M. Koizumi, K. Morita, M. Daigo, S. Tsutsumi, K. Abe, S. Obika, T. Imanishi, *Nucleic Acids Res.* 2003, *31*, 3267–3273.

[19] T. Hojland, B. R. Babu, T. Bryld, J. Wengel, *Nucleosides Nucleotides Nucleic Acids* 2007, *26*, 1411–1414.

[20] U. V Schneider, N. D. Mikkelsen, N. Jøhnk, L. M. Okkels, H. Westh, G. Lisby, *Nucleic Acids Res.* 2010, *38*, 4394–4403.

[21] D. A. Collier, T. Nguyen Thanh, C. Helene, *J. Am. Chem. Soc.* 1991, *113*, 1457–1458.

[22] G. C. Silver, J.-S. Sun, C. H. Nguyen, A. S. Boutorine, E. Bisagni, C. Hélène, *J. Am. Chem. Soc.* 1997, *119*, 263–268.

[23] C. Escudé, C. H. Nguyen, S. Kukreti, Y. Janin, J.-S. Sun, E. Bisagni, T. Garestier, C. Hélène, *Proc. Natl. Acad. Sci. U.S.A.* 1998, *95*, 3591–3596.

[24] V. Tähtinen, L. Granqvist, P. Virta, *Bioorg. Med. Chem.* 2015, *23*, 4472–4480.

[25] L. Granqvist, V. Tähtinen, P. Virta, *Molecules 2019, Vol. 24, Page 580* 2019, *24*, 580.

[26] M. Hebenbrock, J. Müller, *Comprehensive Inorganic Chemistry III, Third Edition* 2023, *1–10*, 664–713.

[27] S. Naskar, R. Guha, J. Müller, *Angew. Chem. Int. Ed.* 2020, *59*, 1397–1406.

[28] J. Müller, *Coord. Chem. Rev.* 2019, *393*, 37–47.

[29] B. Jash, J. Müller, *Chem. Eur. J.* 2017, *23*, 17166–17178.

[30] Y. Takezawa, J. Müller, M. Shionoya, *Chem. Lett.* 2017, *46*, 622–633.

[31] T. Dairaku, K. Furuita, H. Sato, J. Sebera, K. Nakashima, A. Ono, V. Sychrovsky, C. Kojima, Y. Tanaka, *Inorg. Chim. Acta* 2016, *452*, 34–42.

[32] S. Taherpour, O. Golubev, T. Lönnberg, *Inorg. Chim. Acta* 2016, *452*, 43–49.

[33] M. K. Graham, T. R. Brown, P. S. Miller, *Biochemistry* 2015, *54*, 2270–2282.

[34] M. A. Campbell, P. S. Miller, *Bioconjug. Chem.* 2009, *20*, 2222–2230.

[35] C. Colombier, B. Lippert, M. Leng, *Nucleic Acids Res.* 1996, *24*, 4519–4524.

[36] B. Lippert, M. Leng, in *Metallopharmaceuticals I* (Eds.: M. Clarke, P. Sadler), Springer Berlin Heidelberg, 1999, pp. 117–142.

[37] C. Paris, F. Geinguenaud, C. Gouyette, J. Liquier, J. Lacoste, *Biophys. J.* 2007, *92*, 2498–2506.

[38] T. Ihara, T. Ishii, N. Araki, A. W. Wilson, A. Jyo, *J. Am. Chem. Soc.* 2009, *131*, 3826–3827.

[39] D. U. Ukale, T. Lönnberg, *ChemBioChem* 2018, *19*, 1096–1101.

[40] J. Hennessy, B. McGorman, Z. Molphy, N. P. Farrell, D. Singleton, T. Brown, A. Kellett, *Angew. Chem. Int. Ed.* 2022, *61*, e202110455.

[41] M. K. Graham, P. S. Miller, *J. Biol. Inorg. Chem.* 2012, *17*, 1197–1208.

[42] V. Marchán, A. Grandas, in *Metal Complex–DNA Interactions*, John Wiley & Sons, Ltd, 2009, pp. 273–300.

[43] S. K. Sharma, L. W. McLaughlin, *J. Inorg. Biochem.* 2004, *98*, 1570–1577.

[44] S. K. Sharma, L. W. McLaughlin, *J. Am. Chem. Soc.* 2002, *124*, 9658–9659.

[45] D. U. Ukale, T. Lönnberg, *Angew. Chem. Int. Ed.* 2018, *57*, 16171–16175.

[46] A. Ohkubo, K. Yamada, Y. Ito, K. Yoshimura, K. Miyauchi, T. Kanamori, Y. Masaki, K. Seio, H. Yuasa, M. Sekine, *Nucleic Acids Res.* 2015, *43*, 5675–5686.

[47] C.-Y. Huang, G. Bi, P. S. Miller, *Nucleic Acids Res.* 1996, *24*, 2606–2613.

[48] I. Kumpina, N. Brodyagin, J. A. Mackay, S. D. Kennedy, M. Katkevics, E. Rozners, *J. Org. Chem.* 2019, *84*, 13276–13298.

[49] H. Okamura, Y. Taniguchi, S. Sasaki, *Angew. Chem. Int. Ed.* 2016, *55*, 12445–12449.

[50] D. Guianvarc'h, J. L. Fourrey, R. Maurisse, J. S. Sun, R. Benhida, *Org. Lett.* 2002, *4*, 4209–4212.

[51] D. Guianvarc'h, R. Benhida, J. L. Fourrey, R. Maurisse, J. S. Sun, *Chem. Commun.* 2001, *1*, 1814–1815.

[52] D. U. Ukale, P. Tähtinen, T. Lönnberg, *Chem. Eur. J.* 2020, *26*, 2164–2168.

[53] T. K. Kotammagari, P. Tähtinen, T. Lönnberg, *Chem. Eur. J.* 2022, *28*, e202202530.

[54] H. Liu, C. Cai, P. Haruehanroengra, Q. Yao, Y. Chen, C. Yang, Q. Luo, B. Wu, J. Li, J. Ma, J. Sheng, J. Gan, *Nucleic Acids Res.* 2017, *45*, 2910–2918.

[55] N. A. Frøystein, E. Sletten, *J. Am. Chem. Soc.* 1994, *116*, 3240–3250.

[56] S. Taherpour, H. Lönnberg, T. Lönnberg, *Org. Biomol. Chem.* 2013, *11*, 991–1000.

[57] E. Meggers, P. L. Holland, W. B. Tolman, F. E. Romesberg, P. G. Schultz, *J Am Chem Soc* 2000, *122*, 10714–10715.

[58] P. Scharf, B. Jash, J. A. Kuriappan, M. P. Waller, J. Müller, *Chem. Eur. J.* 2016, *22*, 295–301.

[59] F. Aboul-Ela, D. Koh, I. Tinoco, F. H. Martin, *Nucleic Acids Res.* 1985, *13*, 4811.

[60] O. P. Schmidt, A. S. Benz, G. Mata, N. W. Luedtke, *Nucleic Acids Res.* 2018, *46*, 6470–6479.

[61] O. P. Schmidt, S. Jurt, S. Johannsen, A. Karimi, R. K. O. Sigel, N. W. Luedtke, *Nat. Commun.* 2019, *10*, 4818.

Entry for the Table of Contents

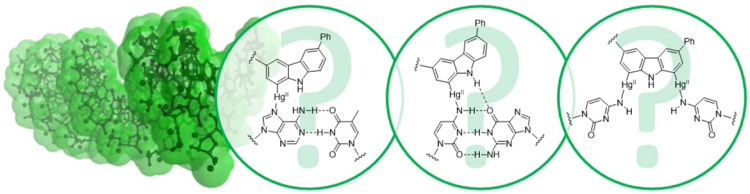

Organomercury derivatives of 6-phenylcarbazole can stabilize triple helices when placed at the termini of triplex-forming homothymine oligonucleotides. In some cases, this stabilization could be attributed to direct coordination of a Hg(II) ion to adenine-N7 or cytosine-N4. For Hg(II)-mediated interaction with both partners of a base pair, the carbazole scaffold would have to be further extended.